Atmospheric Pollution Research 6 (2015) 230-238

Atmospheric Pollution Research

www.atmospolres.com

Spatial distribution and transport patterns of NO_2 in the Tijuana – San Diego area

Claudia Rivera [1], Wolfgang Stremme [2], Hugo Barrera [2,3,4], Martina M. Friedrich [2], Michel Grutter [2], Jose Garcia–Yee [2], Ricardo Torres–Jardon [2], Luis Gerardo Ruiz–Suarez [2]

[1] *Facultad de Ciencias, Universidad Nacional Autónoma de México, Mexico*
[2] *Centro de Ciencias de la Atmósfera, Universidad Nacional Autónoma de México, Mexico*
[3] *Molina Center for Energy and the Environment, La Jolla, CA, USA*
[4] *Department of Earth, Atmospheric and Planetary Sciences, Massachusetts Institute of Technology, Cambridge, MA, USA*

ABSTRACT

The atmospheric composition of the San Diego – Tijuana border is affected by transport of air pollutants between both regions and in both directions. In this study we show NO_2 transport events identified during Cal–Mex 2010 field experiment at two different ground sites, located one downwind of the other. This field campaign was designed to overlap with the closing weeks of CalNex project to observe trans–boundary pollution transport in this area. The measurements showed a clear dispersion pattern of NO_2 towards the east–southeast on several occasions during the field experiment. Additionally, the NO_2 column distribution above the Tijuana – San Diego region was reconstructed from the OMI satellite data product, and a cluster analysis with the corresponding meteorological data was performed to identify four distinct wind patterns yielding different NO_2 distribution maps and detecting dominant wind patterns in this region, either towards the E–SE or E–NE approximately 86% of the time.

Keywords: *NO_2, transport, OMI, cluster, dispersion*

Corresponding Author:
Claudia Rivera
☎ : *+52-55-5622-4972*
🖷 : *+52-55-5622-4841*
✉ : *claudia.rivera@ciencias.unam.mx*

Article History:
Received: 23 May 2014
Revised: 22 August 2014
Accepted: 18 September 2014

doi: 10.5094/APR.2015.027

1. Introduction

The Cal–Mex 2010 field experiment, coordinated by the Molina Center for Strategic Studies on Energy and the Environment, was conducted with the specific focus of characterizing emissions along the California–Mexico border as well as assessing the impact of these emissions on local and regional air quality (Molina et al., 2014). The field campaign was carried out from May 15th to June 30th 2010 and comprised a series of ground sites established along the San Diego – Tijuana border. It was designed to catch and overlap the closing weeks of the CalNex project (ARB, 2008; ARB, 2014). The metropolitan areas share the same air basin, which is basically a coastal plain open to the west and north but closed to the east and south. In general, the terrain increases from sea level along the coast to over 1 200 m a.s.l. (above sea level) inland from the west to east with isolated peaks of about 2 100 m a.s.l. Because of the geographical situation of the region in the Southern California coast, the meteorology and air quality are influenced by the semi–permanent Pacific high and by effects of the coastal marine environment (Bigler–Engler and Brown, 1995).

On the scope of this field experiment, several studies were made during May–June 2010. Based on a review of 10 years of data, Bei et al. (2013) found that between May and June the prevailing wind along the coast is weak and variable between southerly and northerly winds. From sunrise to afternoon, the surface prevailing wind directions along the coast are mainly onshore (southwest to northwest). Toward the nighttime, prevailing winds are weak and diverse, which are similar to the early morning conditions. Zheng et al. (2013a) conducted measurements of formaldehyde, finding that the early onset of the daily maximum was found around 3 h before solar noon, indicating the presence of primary formaldehyde sources and a fast loss due to photolysis in the Tijuana area. The formaldehyde emissions during early morning rush hours were expected to originate from anthropogenic activities, especially from the transportation sector. Shores et al. (2013) characterized the spatial and temporal variability of black carbon in order to identify potential source areas and assess the cross–border transport, finding occurrences of black carbon peaks around midnight. They proposed that black carbon in Tijuana was usually of local origin and that trans–boundary transport from Tijuana into the US was common. Takahama et al. (2013) studied submicron organic aerosols in Tijuana, finding contributions from anthropogenic combustion, biomass burning and marine sources. This study also found that the more oxygenated fraction of the submicron organic aerosol mass was likely to be aged aerosol transported to Tijuana from pollution advected to sea by a sub–grid scale land–sea breeze circulation off the coast of Southern California. Rivera et al. (2013a) quantified nitrogen dioxide (NO_2) fluxes from Tijuana and the Rosarito power plant during Cal–Mex 2010 finding high variability in fluxes and good agreement between modeled and measured plumes. Zheng et al. (2013b) studied volatile organic compounds (VOCs) in Tijuana, attributing them to solvent usage, gas/diesel vehicle

exhausts and aged plumes. Both gasoline and diesel engine emissions were associated with air masses passing through San Ysidro and Otay Mesa, two important cross–border ports. In addition, aged plumes consisting mainly of NO_2 (92%) and long–lived oxygenated VOCs such as methanol and acetone were associated with north–westerly winds, likely from air masses of the San Diego area.

This work focuses on NO_2, one of the most important air pollutants in the troposphere. Nitrogen oxides (NO_X=NO+NO_2) can be emitted from high–temperature combustion processes, such as those occurring in trucks, cars and power plants. However, much of the NO_2 present in the atmosphere is produced through reactions of NO with ozone (O_3) close to the NO_X emissions site, and organic radicals present along the trajectory path where urban plumes are dispersing (Finlayson–Pitts and Pitts, 2000). Nitrogen dioxide has a relatively short lifetime and is a key precursor of O_3 production in the lower atmosphere. Over the Tijuana – San Diego region, anthropogenic emissions from fossil fuel combustion of automobiles, power plants, or industries constitute the main source of nitrogen oxides (NO_X).

According to the most recent emission inventory for the Tijuana Metropolitan Area in 2010, which corresponds to the base year 2005, the NO_X emission was 22.9 kT yr^{-1} (LT Consulting, 2010). On the other hand, the estimated NO_X emissions for the San Diego air basin for the year 2010 are 43.8 kT yr^{-1} (CARB, 2014a). In general, the hourly levels of NO_2 in Tijuana have been below 50 ppb since 2005, although occasional peaks of around 200 ppb are still observed (SPA, 2011). NO_2 hourly average peaks of around 120 ppb have been occasionally observed in San Diego since 2005 (CARB, 2014b).

This paper focuses on NO_2 events (from ground–based measurements) of abnormally large enhancements with respect to the typical levels observed during the Cal–Mex 2010 field experiment. It is of special interest to identify specific days and associate them with prevailing wind schemes to generate maps for the area of interest of the NO_2 vertical–column distribution. For this, data from the Ozone Monitoring Instrument (OMI) onboard the Aura satellite (NASA) was used. Four distinctive maps associated to different wind patterns resulted from a cluster analysis of historic meteorological data.

2. Methodology

2.1. Measurement sites

From May 17th to June 30th 2010 ground–based NO_2 DOAS (Differential Optical Absorption Spectroscopy), NO–NO_2–NO_X concentration and meteorological measurements were conducted at the Parque Morelos (PQM) site which was considered as the super–site for the Cal–Mex 2010 field experiment. The PQM site is located near the urban center of Tijuana (Baja California, Mexico) at 32.50°N, 116.94°W and has an elevation of 47 m a.s.l. (Figure 1). It is about 5.6 km to the south of the Mexico–California border and about 16 km to the western coastline. The site is located in the east of the city, 50 m north of a main avenue and about 300 m to the south of a small hill range. Additional ground–based concentration measurements of NO_X and meteorological parameters were conducted at the Universidad Tecnologica de Tijuana (UTT) located at 32.46°N, 116.82°W at an elevation of 173 m a.s.l. in the western piedmont of the La Gloria mountain range. UTT is about 12 km to the southeast of PQM in the edge of the Tijuana city and about 11 km to the south of the border. Meteorological data from nine stations located in and around the Tijuana and San Diego areas were used to investigate the historic wind patterns of the region. Figure 1 shows the location of all the sites. The period of meteorological data analyzed ranges from 1993 to 2010.

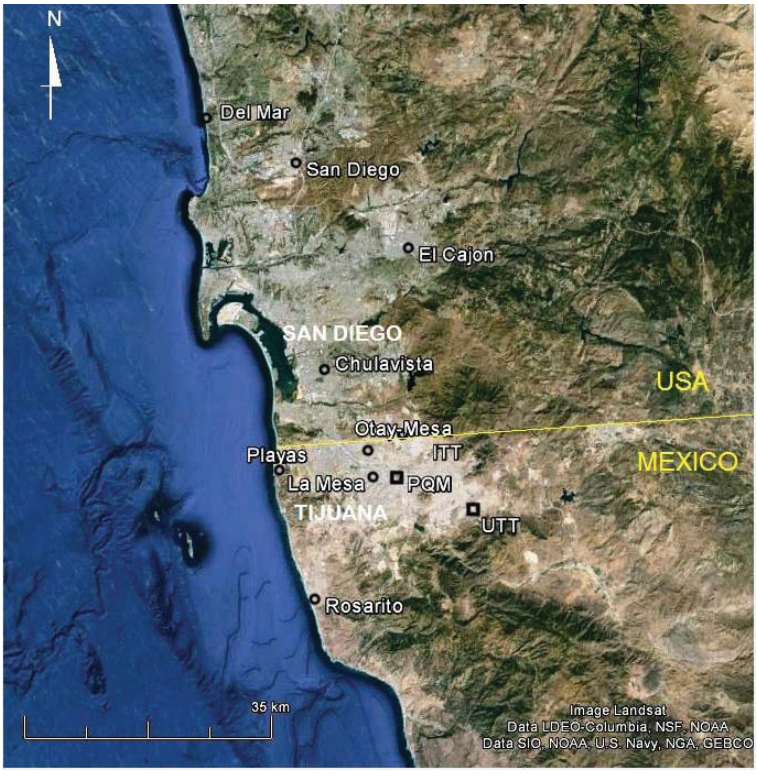

Figure 1. *Spatial distribution of ground–based measurement sites (◘ Cal–Mex 2010 monitoring sites, ○ meteorological stations).*

2.2. Ground–based DOAS measurements

From May 17th to June 30th 2010 ground–based DOAS measurements were conducted at PQM. A spectrometer (Ocean Optics, TR2000) covering the wavelength range of 280–500 nm and with a spectral resolution of ~0.6 nm was coupled to a telescope by means of an optical fiber. Zenith–scattered sunlight spectra were collected and averaged every 20 seconds using the DOASIS software (Kraus, 2006) and further analyzed utilizing the QDOAS fitting code (Fayt et al., 2011).

NO_2 retrievals were conducted in the 405–465 nm wavelength range with a fixed reference spectrum measured on 18 May 2010 at 12:00 local time (LT). This reference spectrum was chosen because it had a low NO_2 content and was measured on a relatively clean day and under clear sky conditions. In the analysis, differential cross–sections of NO_2 at 294 K (Vandaele et al., 1998), O_3 at 221 K and 241 K (Burrows et al., 1999), O_4 – the oxygen dimer– (Hermans et al., 1999) and a Ring spectrum, generated at 273 K from a high resolution Kurucz file using the QDOAS software (Fayt et al., 2011) were included. The measured slant column densities (SCD) need to be converted via an air mass factor (AMF), see e.g. Solomon et al. (1987) for details about the AMF concept, to vertical column densities (VCD). The AMF, defined as the ratio between SCD and VCD, is highly dependent on aerosol properties, such as the single scattering albedo and the phase function form. Chen et al. (2009) performed various radiative transfer (RT) simulations to conduct a case study exploring a wide range of parameter space for AMF calculations for zenith sky DOAS measurements. In the range 0–60 degree SZA, the curve shape of 1/cos(SZA) is comparable to their simulations; however over wide ranges it is below the RT simulation results. Since we did not have sufficient aerosol property information, we decided to limit our observations to times where SZA<60 degree and use 1/cos(SZA) as an AMF.

2.3. Satellite observations

OMI is on–board the NASA Earth Observation System (EOS) – Aura satellite, which follows a sun–synchronous polar orbit (705 km altitude), with an ascending equator crossing at 1:45 PM. Covering a spectral region of 264–504 nm and with an approximate resolution of 0.42–0.63 nm, OMI conducts atmospheric chemistry measurements since 2004 viewing towards the nadir. OMI observations provide complete global coverage in one day with a nominal ground footprint of 13 x 24 km^2 (OMI Team, 2009). Its products include a number of air quality components such as NO_2, SO_2, BrO, HCHO, as well as the aerosol optical depth (Levelt et al., 2006a; Levelt et al., 2006b).

Bucsela et al. (2006) describe in detail the OMI operational algorithm, which is based on the DOAS method (Platt and Stutz, 2008) for the evaluation of spectra. In this method, a spectral fit is applied to all measured spectra, providing results on SCDs for each OMI pixel. Afterwards, the computed SCDs are converted to VCDs using an AMF as described in Bucsela et al. (2006).

In this work, the OMNO2 Level 2 collection number 003 algorithm version 1.1.4.4 data product was used to conduct the analysis. We have considered total NO_2 columns from cloud fraction below 20% for 2006 to 2011. This dataset has been reprocessed and released on December 2011 (Claas, 2012).

2.4. Reconstruction of the mean column NO_2 distribution

The mean column NO_2 distribution over a 2 km grid was reconstructed from measurements done on a larger footprint (13× 24 km^2 for the OMI dataset), solving the mathematically ill–posed problem $Y = Kx+\mathcal{E}$. In this equation Y represents the vector containing all OMI NO_2 measurements, x is the solution vector which contains the estimate of the mean column NO_2 distribution on the chosen grid, $\mathcal{E}$ represents the deviation between a column measured or retrieved from the space measurement and the estimated mean value. $\mathcal{E}$ is mainly dependent on the day–to–day variance, but also on the seasonal variance and measurement precision. The matrix K describes how the measurements are related with the mean gas horizontal distribution and represents a forward model that reproduces the footprint of the OMI instrument (13 × 24 km^2 at nadir). The reconstruction algorithm uses a Tihkonov–smoothing–constraint, similar to the one used for vertical profile retrievals or in image restoration algorithms. The method has already been applied for the reconstruction of seasonal and annual mean distributions of NO_2 and CO near Mexico City and further details of this method can be found in Rivera et al. (2013b) and Stremme et al. (2013).

2.5. Ground–based gas concentration measurements

The ground–based measurements of NO_X at PQM and UTT were measured with chemiluminescence $NO/NO_X/NO_2$ analyzers (Thermo Environmental Instruments Technology 42C), which are non–specific for NO_2 with a detection limit of 0.4 ppbv and a precision of 1 ppbv. At PQM, the instrument was placed inside the CCA–UNAM air quality mobile monitoring station, while at UTT, the analyzer was inside an integrated AirPointer multi–gas measurement platform (Recordum Messtechnik GmbH, Austria). The inlet sampling manifold was set at around 5 m above the ground at both sites. Both instruments were calibrated by the Centro Nacional de Investigacion y Capacitacion Ambiental (CENICA, INE) following U.S. EPA protocols before, during and after the campaign using NIST (National Institute of Standards and Technology) certified gas mixtures, which were prepared with an API M700 Calibrator equipped with an internal ozone generator and a zero air supply (Thermo Environmental Instruments, Model 111). The information was registered from the instruments in 5–min averages.

2.6. Ceilometer data

Backscattered light at PQM was measured using a Vaisala CL31 ceilometer, an active instrument based on the LIDAR (light detection and ranging) measurement technique. The measurement principle involves the transmission of pulsed laser radiation into the atmosphere, which is then backscattered and detected at a certain time delay. The measurement range of the instrument used in this field study was from 0 up to 7 500 m with a 10 m resolution. The LIDAR wavelength of 905 nm was provided by an InGaAs MOCVD laser diode, 110 ns, 1.2 µJ per pulse, operating at 8.2 kHz. Estimates of the mixing layer height were retrieved using the gradient method in the CL31 MLH software, following the methodology described by Munkel et al. (2007). This method is focused on selecting the maximum of the negative gradient of the backscatter coefficient to be the top of the mixed layer.

2.7. Radiosondes

During the Cal–Mex 2010 campaign, 50 GRAW DFM–06 radiosondes were launched from a clear area near the mobile unit at PQM, providing data of atmospheric pressure, temperature, humidity, wind speed and direction from the surface and up to several kilometers. Two radiosondes were launched per day at the local daylight saving times (LT, UTC + 7) 07:00 and 19:00. However, after May 31th, the launching schedule changed to 07:00 and 15:00 (LT).

2.8. Historic meteorological dataset

Historical data analysis was performed for Tijuana and San Diego regions based on the EPA´s Air Quality System (AQS) repository of ambient air quality and meteorological data, from January 1993 to December 2010. The datasets from AQS contain ambient air pollution and meteorological information collected by United States and Mexican monitoring stations. The location of the 9 stations around the Tijuana and San Diego areas used for this study are shown in Figure 1. Datasets of meteorological

parameters consist of temperature, barometric pressure, wind speed and wind direction scalar, and wind direction and wind speed resultant (using instrumental vector summation).

2.9. Cluster analysis of meteorological data

The unfiltered trace gas distribution from the OMI dataset averaged over a large time period is expected to reflect the general distribution from various dispersion patterns emerging from stationary or periodic sources such as industry, the traffic on roads, boats, etc. Therefore, the classification into groups with different wind pattern should result in distinctive trace gas distributions. A similar approach was used e.g. in Beirle et al. (2011). Based on the historic data from meteorological sites (see Section 2.8), groups of days with characteristically different daily wind patterns in the study area were identified by cluster analysis.

The cluster analysis can be realized in different ways. One way is to use time–averaged information from each station separately, resulting in an 18 dimensional space for the cluster analysis. Alternatively, the dimensions of the vectors can be reduced by averaging over various monitoring sites. In the former case, only days for which meteorological data on all sites are available could be classified, so that either only few meteorological sites or only few satellite measurements could contribute to the analysis. On the other hand, if the daily mean over various sites of zonal and meridional wind components are calculated, the lack of data in a particular site is not crucial and the strategy allows for the use of all available measurements in the area of study. Using a larger dataset reduces the noise, which originates from day–to–day variations, however, this requires that measurements on different sites are correlated so that they can be averaged without losing important information.

To characterize the wind pattern, we use the wind velocity in two–dimensional Cartesian coordinates measured at nine different locations between 11 and 15 hours local time (see Figure 1). In a first step, we perform a cluster analysis where each data point is described by 18 coordinates corresponding to the 9 local Cartesian coordinate pairs.

The cluster analysis was performed using a K–means algorithm (we used the K–means and silhouette implementations from Matlab version 2013a, Natick, Massachusetts: The MathWorks Inc., 2013) which reduces the sum over the variances in each cluster. As distance measure, the squared Euclidean distance was used. In order to find the global minimum, we used 100 different seeds for the initial cluster centers.

Since the number of clusters is a free parameter, we tried different numbers of clusters and evaluated the quality of the separation using silhouette plots, where the silhouette value for each data point is a measure for the affinity of the point to its cluster. This value is normalized to values between –1 and 1. Negative values indicate that a point is on average closer to points in another cluster than to points in its own cluster; positive values close to one indicate a small distance to points in the corresponding cluster compared to the distance to points in other clusters and hence indicate a good separation. Using four cluster centers resulted in the best separation.

In a second step, we characterized each point by two coordinates, corresponding to the averaged wind velocity over the nine stations. We again performed a cluster analysis in this two–dimensional space and found that 93.6% of the data points were classified as belonging to the same clusters as in the cluster analysis in 18 dimensions. Further, we find that the average of the silhouette value of the points that changed cluster (0.065) is an order of magnitude smaller than the overall average silhouette value (0.45), indicating that the data points that changed cluster where those that were located at the cluster borders. Using the averages also results in a higher average silhouette value (0.53). We therefore argue that the use of the averaged wind velocity over the nine stations to identify days with similar wind pattern is legitimate. As mentioned, the advantage of this strategy is that data from days where wind velocity data is not available at all 9 stations can be included in the averaging. This increases the data set from 3 377 days at which data at all nine stations is available to the full 18 year record (6 573 days).

3. Results and Discussion

3.1. Ground–based measurements

Analysis of differential vertical NO_2 column and surface concentration measurements during the field experiment denoted specific days when a clear enhancement of NO_2 columns over both PQM and UTT sites were detected. Of special interest are days when a time delay of the daily maximum is observed between the two sites. The five days during the field campaign that showed this behavior were 3, 7, 17, 18 and 25 June (Figure 2). The time delay of the daily maximum for these five days was 50 to 185 minutes. Depending on meteorological conditions, this is the expected transport time between the two sites for typical wind speeds between 1 and 4 m s^{-1} (1 m s^{-1} = 1.94384 knots) which were frequently observed during the field campaign (Bei et al., 2013). For the sake of comparison, NO_2 columns from the DOAS measurements were converted to surface concentrations assuming a well–mixed lower layer (Volten et al., 2009; Sluis et al., 2010) (height measured by ceilometer, see Section 2.6) and correcting for pressure and temperature.

On all occasions the NO_2 concentrations calculated from DOAS measurements were higher than the concentrations measured at ground level, which may be an indication that the transported plumes did not completely reach the surface. In an urban environment, higher concentrations of pollutants are expected to be located close to the ground, as Dieudonne et al. (2013) found in Paris. In situations where the polluted air masses have larger concentrations at higher altitudes, surface concentrations measured by ground–based instruments will be lower or hardly detected. However, the DOAS instrument pointing towards the zenith will have the ability to quantify the complete atmospheric column, as described by Melamed et al. (2009). Since we use a simplified AMF for the VCD calculation, a higher apparent column may also be due to multi–scattering effects particularly in plumes containing high particulate matter or/and humidity. A comparison to the radiative transfer simulations from Chen et al. (2009), suggests that an AMF of 1/cos(SZA) is likely to be of the order of 0.1 too low. Therefore, it is likely that the DOAS VCDs are of the order of 10% too high and hence are the estimated surface concentrations. It should also be mentioned that the NO_2 concentrations calculated from DOAS measurements and the measured NO_2 concentrations show an excellent coincidence among them regarding the time when the highest values occur during the day. They also decreased in magnitude from the PQM monitoring site to the one located at UTT, as would be expected from a downwind dispersion of a reacting urban plume where part of both, the primary NO_2 picked up along the path of the air mass transport, and of secondary NO_2 produced from the NO oxidation in the dispersing plume is rapidly removed by its conversion to other species such as HNO_3 and nitrate aerosols. Measurements of NO_Z species which included HNO_3 at PQM during Cal–Mex exhibited higher concentrations in the early morning, indicating a larger NO_X oxidation (Zheng et al., 2013b). In addition, real time measurements of the aerosols composition in the same site showed that in general nitrate aerosols peaked during morning hours (Takahama et al., 2013). It is worth noting that on all days when a clear NO_2 concentration enhancement was detected along with a certain time delay between the two monitoring sites, the wind direction from the ground to the mixing layer height indicates winds blowing from the north–west and towards both PQM and UTT monitoring sites (Figure 2b, 2d, 2f, 2h, 2j).

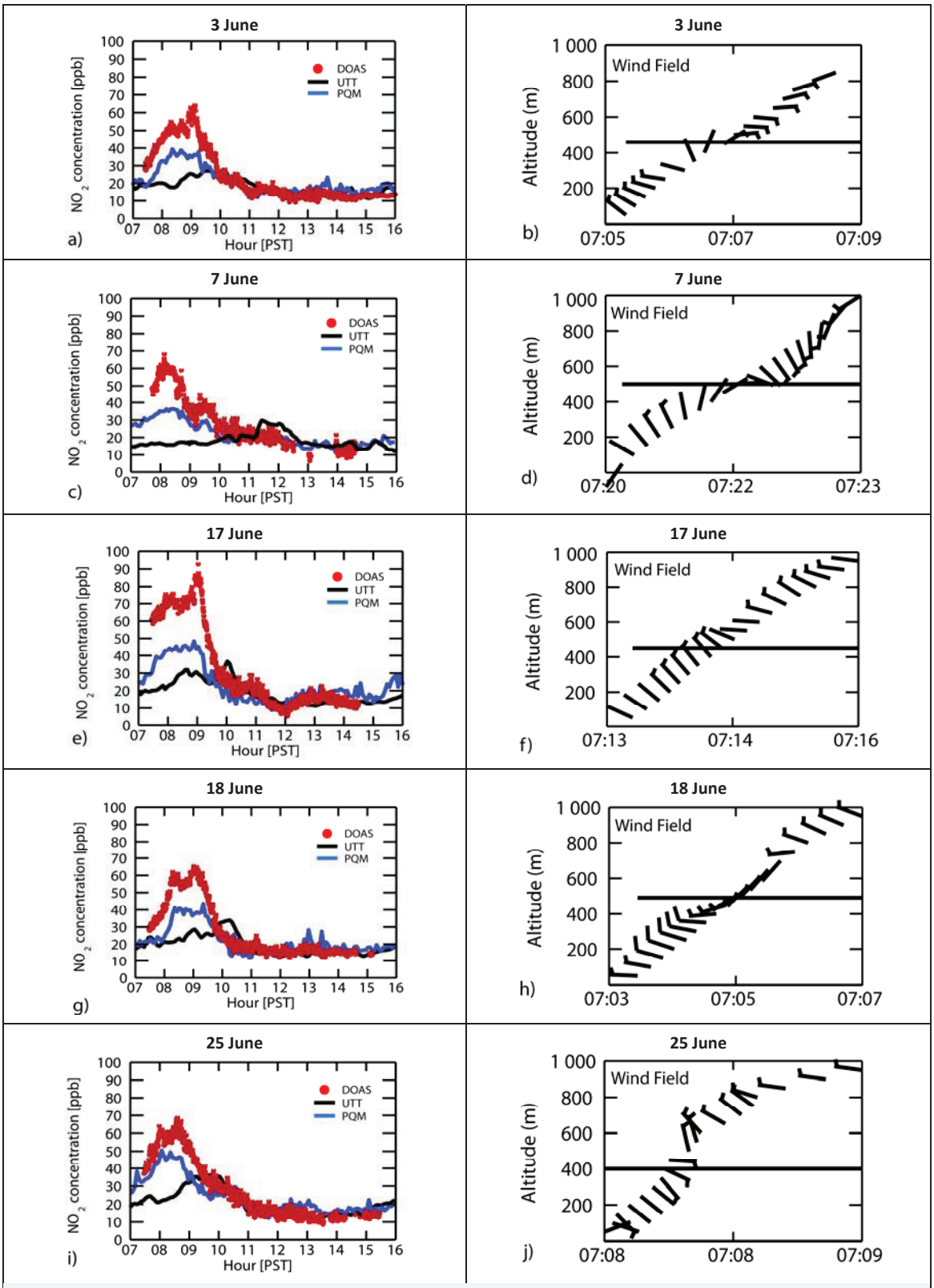

Figure 2. *NO_2 concentration measurements (in ppbv) conducted at UTT (black solid line), at PQM (blue solid line) and NO_2 concentration calculated from column measurements conducted at PQM (red circles) measured on 3 June **(a)**, 7 June **(c)**, 17 June **(e)**, 18 June **(g)** and 25 June **(i)**. Right panels **(b)**, **(d)**, **(f)**, **(h)**, **(j)** are windfield plots constructed from radiosonde data showing wind direction and wind speed (barbs represent wind speed in knots: a short barb represents 5 knots while each long barb represents 10 knots) as a function of altitude launched on the same dates at 7:00 LT. The measured mixing layer height from the ceilometer is shown as a black horizontal line.*

On two specific days (31 May and 19 June) of the field campaign, an NO_2 concentration enhancement was observed. How-ever, no time delay was identified between both PQM and UTT monitoring sites (Figure 3a, 3c). On these two specific days, NO_2 concentrations calculated from DOAS measurements were also higher than ground–level measured concentrations. Also, both days were characteristic of opposite wind patterns, with winds blowing predominately from the southeast on 31 May and winds blowing from the northwest on 19 June (Figure 3b, 3d).

3.2. OMI NO_2 distribution over the Tijuana – San Diego border region

Four specific meteorological patterns were identified from the cluster analysis results (see Section 2.9) of the analyzed historic meteorological data (see Section 2.8). The most common pattern was when winds were blowing towards the east–southeast with 45%, followed by winds heading towards the east–northeast (41%), then the third pattern identified with winds blowing towards the north–northeast (10%) and finally, the fourth identified pattern suggested winds blowing towards the west, with only 4% occurrence. Figure 4 depicts the cluster centers (black cross) and Table 1 gives a summary of the cluster analysis and its corresponding wind directions as well as number of occurrences. Figure 5 shows a histogram of the wind patterns distribution over the months of the year for each of the four clusters. From Figure 5 it is possible to infer that wind patterns corresponding to cluster (a) are more frequently present during March, April, July, August, September, October and November. Wind patterns characteristic of cluster (b) are present during May, June, and July. January and February are the months that contribute more importantly to cluster (c), while December and January are the months that contribute to cluster (d).

Table 1. *Cluster analysis results, number of occurrences and its corresponding wind dispersion pattern*

Cluster	Number of Occurrences	Frequency (%)	Dispersion Pattern
a	2 976	45	Towards east-southeast
b	2 699	41	Towards east-northeast
c	634	10	Towards north-northeast
d	264	4	Towards west

Figure 6 shows NO_2 total column distribution maps constructed from measurements conducted by the OMI instrument between 2006 and 2011 and classified according to the four clusters defined above. A clear NO_2 column footprint can be observed over the San Diego – Tijuana metropolitan area particularly during the most frequent meteorological conditions favoring transport of pollutants towards the east–southeast and east–northeast (a and b), which together correspond to 86% of the days. An overall stronger enhancement is observed when the east–southeast wind pattern is present (a). On the few occasions when the meteorological conditions bring pollutants towards the north–northeast (c), a well defined but less pronounced enhancement of NO_2 results along the border region and clearly encompassing both cross–border ports and one clear region southeast of San Diego. During the less frequent (<5%) days when winds are transported towards the west, a very strong enhancement above the Greater San Diego, with some contribution of the Tijuana metropolitan area, is shown to move towards the ocean. It can be inferred from Figure 6 that larger NO_2 columns are measured over San Diego than over Tijuana.

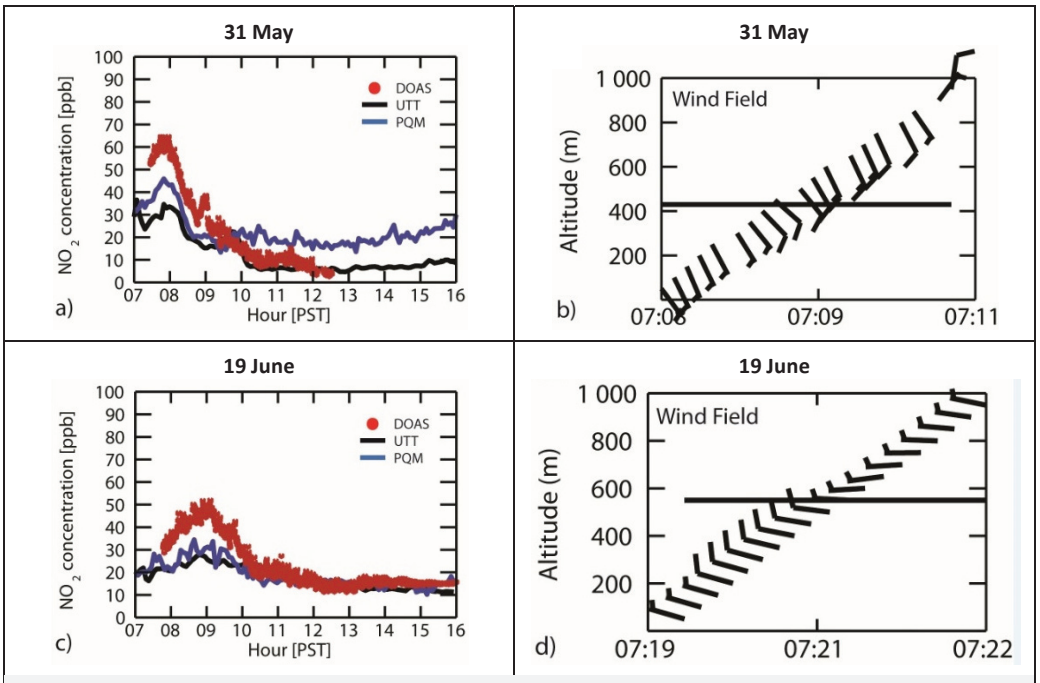

Figure 3. *NO_2 ground–based measurements (in ppbv) conducted at UTT (black solid line), at PQM (blue solid line) and NO_2 concentrations calculated from column measurements conducted at PQM (red circles) measured on 31 May **(a)** and 19 June **(c)**. Right panels **(b), (d)** are windfield plots constructed from radiosonde data showing wind direction and wind speed (barbs represent wind speed in knots: a short barb represents 5 knots while each long barb represents 10 knots) as a function of altitude launched on the same dates. The measured mixing layer height from the ceilometer is shown as a black horizontal line.*

4. Conclusions

In this study we present the analysis of NO_2 measured at two ground sites, one of which was equipped with a DOAS instrument to detect differential vertical columns, during the Cal–Mex field study in May–June 2010. Also, the NO_2 column distribution above the Tijuana – San Diego region was reconstructed from the OMI satellite data product, and a cluster analysis of the historic meteorological data was used to classify the NO_2 maps into four distinct wind patterns. The simultaneous surface measurements at the two sites in the Tijuana area showed that in several days a clear dispersion pattern of NO_2 towards the E–SE was present. These polluted air masses could have been transported aloft from the San Diego metropolitan area according to a time delay in the peaks detected at ground and a comparison with the larger concentrations derived from the DOAS column measurements. Clear enhancements of NO_2 are observed over the entire Tijuana – San Diego metropolitan area according to satellite measurements. A dominant wind pattern is identified towards the E–SE and E–NE favoring the dispersion of pollution from the coastal and urban areas towards the continent. The NO_2 maps were classified according to the main wind patterns and the San Diego region is identified as an important contributor to the high NO_2 events measured in Tijuana during the field study. It is suggested from Figure 6 that larger NO_2 columns are measured over San Diego than over Tijuana. It is nevertheless evident that both San Diego and Tijuana are highly influenced by the transport of pollutants from the Californian southern coast (ARB, 2014) since they share the same air basin, at least regarding NO_X and therefore also on ozone pollution.

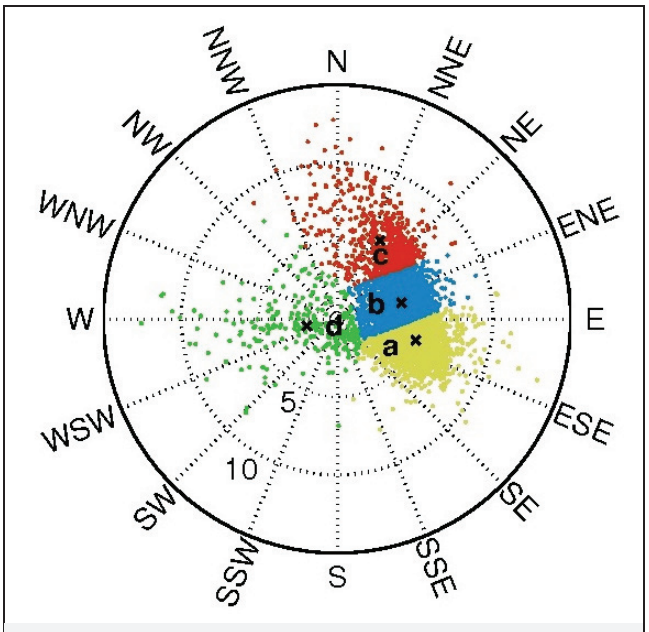

Figure 4. *Results of the cluster analysis conducted based on the historic data (1993–2010) from meteorological sites. The radial axes correspond to wind speed in knots.*

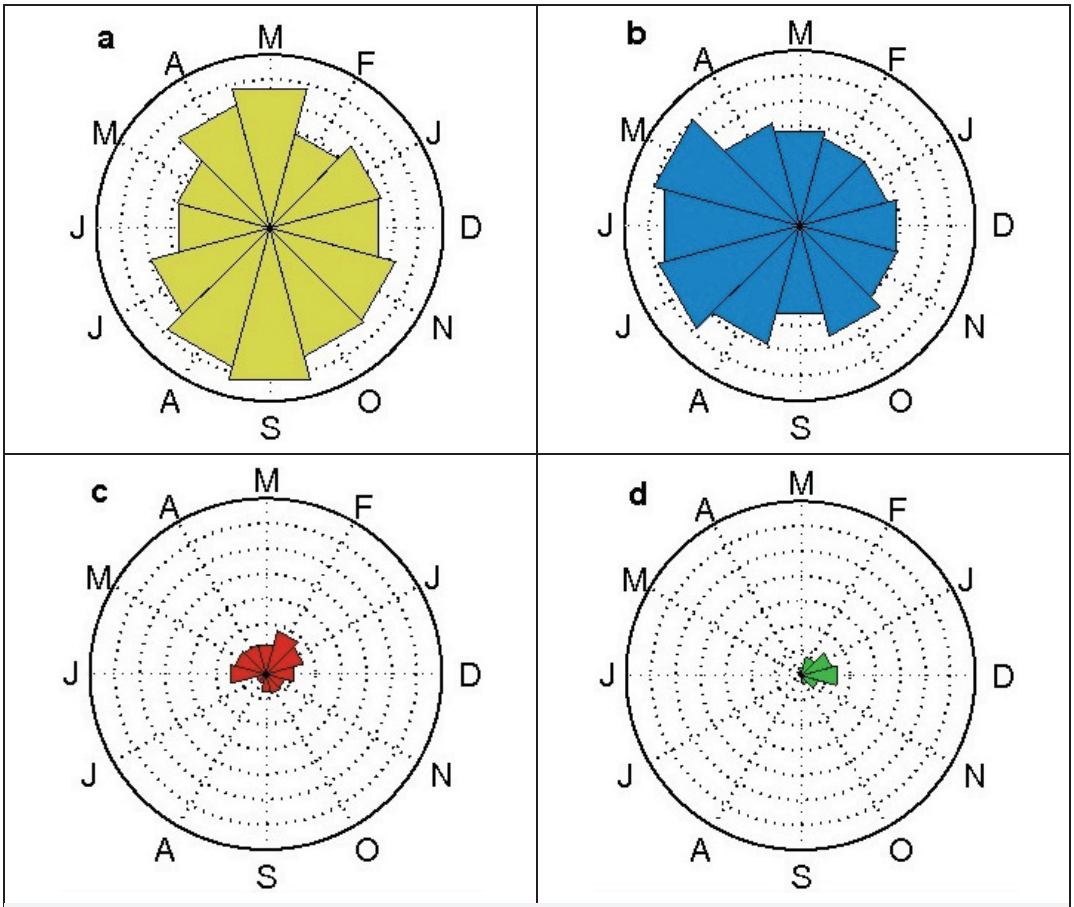

Figure 5. *Histogram of the wind patterns distribution over the months of the year for each of the four clusters. The radial axes correspond to number of occurrences where each dashed circle is 50 occurrences.*

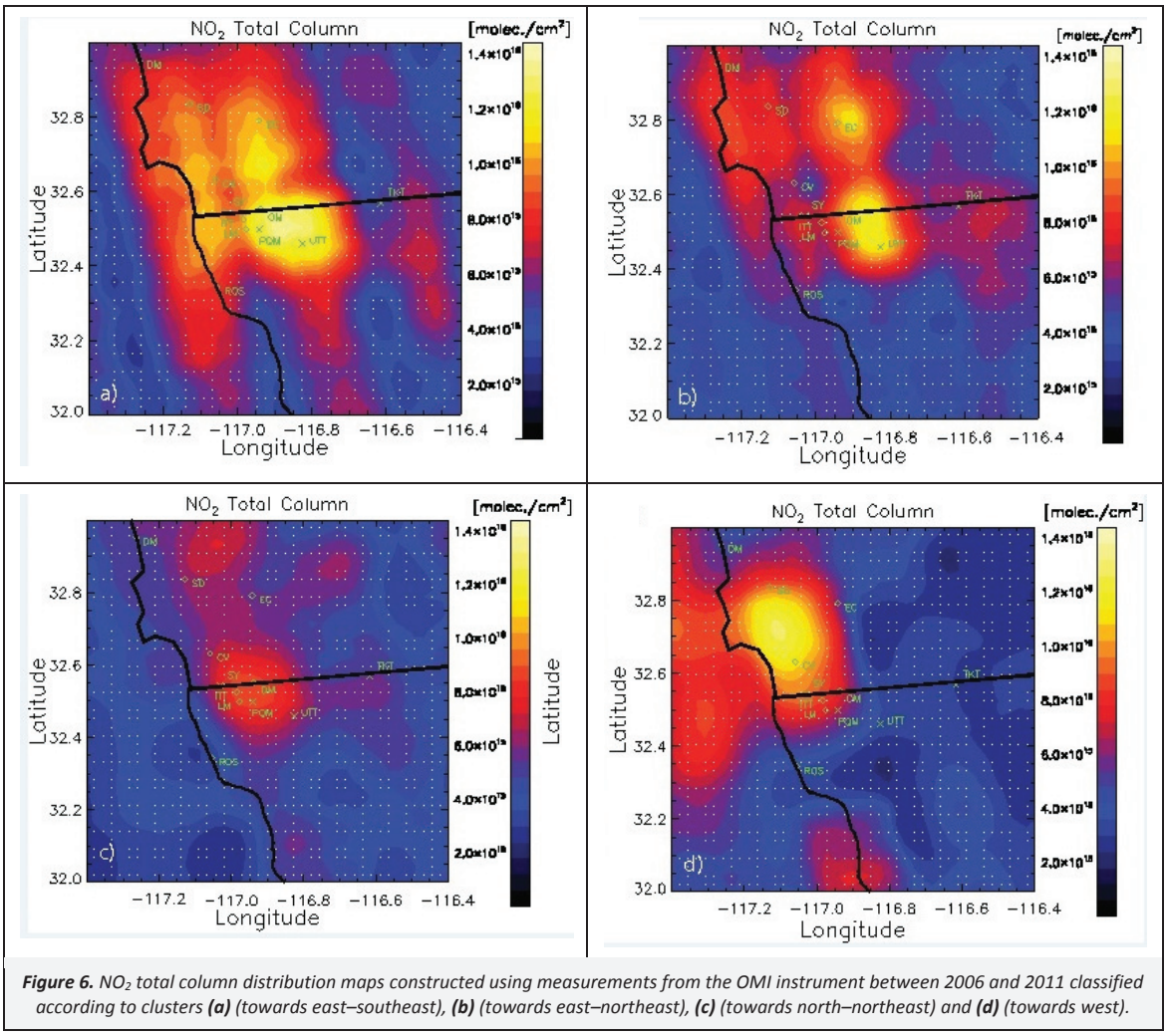

Figure 6. *NO_2 total column distribution maps constructed using measurements from the OMI instrument between 2006 and 2011 classified according to clusters* ***(a)*** *(towards east–southeast),* ***(b)*** *(towards east–northeast),* ***(c)*** *(towards north–northeast) and* ***(d)*** *(towards west).*

Acknowledgments

This work was partially supported by project DGAPA–PAPIIT No. IN109914–3. MMF is grateful for a postdoctoral fellowship provided by DGAPA/UNAM. The OMI project is managed by the Netherlands Agency for Aerospace Programs (NIVR) and the Royal Netherlands Meteorological Institute (KNMI). The authors acknowledge the free use of NO_2 total column data from the OMI sensor accessed via the NASA Aura Validation Data Center (AVDC) and Goddard Earth Science (GES) Data and Information Services Center (DISC). Caroline Fayt and Michel van Roozendael from the Belgian Institute for Space Aeronomie are acknowledged for the free use of the QDOAS software used for the evaluation of the ground–based DOAS data presented in this work. Diana García Payne is thanked for conducting the DOAS measurements. Jorge Alejandro Torres Jaramillo is acknowledged for technical support with the instruments inside the mobile unit. Agustín García from Centro de Ciencias de la Atmósfera (UNAM) is acknowledged for lending the radiosondes receiver used in this study. This project was coordinated by the Molina Center for Strategic Studies on Energy and the Environment.

References

ARB (Air Resources Board), 2014. Synthesis of Policy Relevant Findings from the CalNex 2010 Field Study, Final Report to the Research Division of the California Air Resources Board, ARB Agreement No. 10–326, 205 pages.

ARB (Air Resources Board), 2008. 2010 CalNex White Paper, Research at the Nexus of Air Quality and Climate Change, 12 pages.

Bei, N.F., Li, G.H., Zavala, M., Barrera, H., Torres, R., Grutter, M., Gutierrez, W., Garcia, M., Ruiz–Suarez, L.G., Ortinez, A., Guitierrez, Y., Alvarado, C., Flores, I., Molina, L.T., 2013. Meteorological overview and plume transport patterns during Cal–Mex 2010. *Atmospheric Environment* 70, 477–489.

Beirle, S., Boersma, K.F., Platt, U., Lawrence, M.G., Wagner, T., 2011. Megacity emissions and lifetimes of nitrogen oxides probed from space. *Science* 333, 1737–1739.

Bigler–Engler, V., Brown, H.W., 1995. Analysis of an ozone episode during the San–Diego Air–Quality Study – the significance of transport aloft. *Journal of Applied Meteorology* 34, 1863–1876.

Bucsela, E.J., Celarier, E.A., Wenig, M.O., Gleason, J.F., Veefkind, J.P., Boersma, K.F., Brinksma, E.J., 2006. Algorithm for NO_2 vertical column retrieval from the ozone monitoring instrument. *IEEE Transactions on Geoscience and Remote Sensing* 44, 1245–1258.

Burrows, J.P., Richter, A., Dehn, A., Deters, B., Himmelmann, S., Voigt, S., Orphal, J., 1999. Atmospheric remote–sensing reference data from GOME—2. Temperature–dependent absorption cross sections of O_3 in the 231–794 nm range. *Journal of Quantitative Spectroscopy and Radiative Transfer* 61, 509–517.

CARB (California Air Resources Board), 2014a. Estimated Annual Average Emissions, Emission Data by Air Basin, California Air Resources Board, http://www.arb.ca.gov/app/emsinv/fcemssumcat2013.php, accessed in January 2014.

CARB (California Air Resources Board), 2014b. iADAM: Air Quality Data Statistics, http://www.arb.ca.gov/adam/index.html, accessed in August 2014.

Chen, D., Zhou, B., Beirle, S., Chen, L.M., Wagner, T., 2009. Tropospheric NO_2 column densities deduced from zenith–sky DOAS measurements in Shanghai, China, and their application to satellite validation. *Atmospheric Chemistry and Physics* 9, 3641–3662.

Claas, J.J., 2012. Notes on the Releases of OMI Data Products, KNMI, Issue 1.2, January 24, 2012.

Dieudonne, E., Ravetta, F., Pelon, J., Goutail, F., Pommereau, J.P., 2013. Linking NO_2 surface concentration and integrated content in the urban developed atmospheric boundary layer. *Geophysical Research Letters* 40, 1247–1251.

Fayt, C., De Smedt, I., Letocart, V., Merlaud, A., Pinardi, G., Van Roozendael, M., 2011. QDOAS Software User Manual, Belgian Institute for Space Aeronomie, 71 pages.

Finlayson–Pitts, B.J., Pitts, J.N., 2000. *Chemistry of the Upper and Lower Atmosphere: Theory, Experiments and Applications,* Academic Press, San Diego, pp. 17–18.

Hermans, C., Vandaele, A.C., Carleer, M., Fally, S., Colin, R., Jenouvrier, A., Coquart, B., Merienne, M.F., 1999. Absorption cross–sections of atmospheric constituents: NO_2, O_2, and H_2O. *Environmental Science and Pollution Research (International)* 6, 151–158.

Kraus, S., 2006. *DOASIS: A Framework Design for DOAS*. Ph.D. Thesis, Mannheim University, Mannheim, Germany, 184 pages.

Levelt, P.F., Hilsenrath, E., Leppelmeier, G.W., van den Oord, G.H.J., Bhartia, P.K., Tamminen, J., de Haan, J.F., Veefkind, J.P., 2006a. Science objectives of the Ozone Monitoring Instrument. *IEEE Transactions on Geoscience and Remote Sensing* 44, 1199–1208.

Levelt, P.F., Van den Oord, G.H.J., Dobber, M.R., Malkki, A., Visser, H., de Vries, J., Stammes, P., Lundell, J.O.V., Saari, H., 2006b. The Ozone Monitoring Instrument. *IEEE Transactions on Geoscience and Remote Sensing* 44, 1093–1101.

LT Consulting, 2010. Inventory of atmospheric emissions in the municipalities of Tijuana and Rosarito, Baja California, Final Report, Prepared for: Border Environment Cooperation Commission, U.S. Environmental Protection Agency Region 9 and Baja California Secretariat of Environmental Protection, http://server.cocef.org/Final_Reports_B2012/20081/20081_Final_Report_ES.pdf, accessed in August 2014.

Melamed, M.L., Basaldud, R., Steinbrecher, R., Emeis, S., Ruiz–Suarez, L.G., Grutter, M., 2009. Detection of pollution transport events southeast of Mexico City using ground–based visible spectroscopy measurements of nitrogen dioxide. *Atmospheric Chemistry and Physics* 9, 4827–4840.

Molina, L.T., Russell, L.M., Marr, L.C., 2014. Preface. *Atmospheric Environment* 88, 306–307.

Munkel, C., Eresmaa, N., Rasanen, J., Karppinen, A., 2007. Retrieval of mixing height and dust concentration with lidar ceilometer. *Boundary–Layer Meteorology* 124, 117–128.

OMI Team, 2009. Ozone Monitoring Instrument (OMI) Data User's Guide, OMI–DUG–3.0.

Platt, U., Stutz, J., 2008. *Differential Optical Absorption Spectroscopy (DOAS): Principle and applications*, Springer, Heidelberg, Germany, pp. 135–174.

Rivera, C., Barrera, H., Grutter, M., Zavala, M., Galle, B., Bei, N.F., Li, G.H., Molina, L.T., 2013a. NO_2 fluxes from Tijuana using a mobile mini–DOAS during Cal–Mex 2010. *Atmospheric Environment* 70, 532–539.

Rivera, C., Stremme, W., Grutter, M., 2013b. Nitrogen dioxide DOAS measurements from ground and space: Comparison of zenith scattered sunlight ground–based measurements and OMI data in central Mexico. *Atmosfera* 26, 401–414.

Shores, C.A., Klapmeyer, M.E., Quadros, M.E., Marr, L.C., 2013. Sources and transport of black carbon at the California–Mexico border. *Atmospheric Environment* 70, 490–499.

Sluis, W.W., Allaart, M.A.F., Piters, A.J.M., Gast, L.F.L., 2010. The development of a nitrogen dioxide sonde. *Atmospheric Measurement Techniques* 3, 1753–1762.

Solomon, S., Schmeltekopf, A.L., Sanders, R.W., 1987. On the interpretation of zenith sky absorption–measurements. *Journal of Geophysical Research–Atmospheres* 92, 8311–8319.

SPA (Secretariat of Environmental Protection), 2011. Program to Improve Air Quality in the Metropolitan Area of Tijuana, Tecate and Rosarito 2012–2020, Secretariat of Environmental Protection, Baja California State Government, Ministry of Environment and Natural Resources, http://www.semarnat.gob.mx/archivosanteriores/temas/gestionambiental/calidaddelaire/Documents/ProAire%20ZMT2.pdf, accessed in May 2014.

Stremme, W., Grutter, M., Rivera, C., Bezanilla, A., Garcia, A.R., Ortega, I., George, M., Clerbaux, C., Coheur, P.F., Hurtmans, D., Hannigan, J.W., Coffey, M.T., 2013. Top–down estimation of carbon monoxide emissions from the Mexico Megacity based on FTIR measurements from ground and space. *Atmospheric Chemistry and Physics* 13, 1357–1376.

Takahama, S., Johnson, A., Morales, J.G., Russell, L.M., Duran, R., Rodriguez, G., Zheng, J., Zhang, R., Toom–Sauntry, D., Leaitch, W.R., 2013. Submicron organic aerosol in Tijuana, Mexico, from local and Southern California sources during the CalMex campaign. *Atmospheric Environment* 70, 500–512.

Vandaele, A.C., Hermans, C., Simon, P.C., Carleer, M., Colin, R., Fally, S., Merienne, M.F., Jenouvrier, A., Coquart, B., 1998. Measurements of the NO_2 absorption cross–section from 42 000 $cm^{(-1)}$ to 10 000 $cm^{(-1)}$ (238–1 000 nm) at 220 K and 294 K. *Journal of Quantitative Spectroscopy & Radiative Transfer* 59, 171–184.

Volten, H., Brinksma, E.J., Berkhout, A.J.C., Hains, J., Bergwerff, J.B., Van der Hoff, G.R., Apituley, A., Dirksen, R.J., Calabretta–Jongen, S., Swart, D.P.J., 2009. NO_2 lidar profile measurements for satellite interpretation and validation. *Journal of Geophysical Research–Atmospheres* 114, art. no. D24301.

Zheng, J., Zhang, R., Garzon, J.P., Huertas, M.E., Levy, M., Ma, Y., Torres–Jardon, R., Ruiz–Suarez, L.G., Russell, L., Takahama, S., Tan, H., Li, G., Molina, L.T., 2013a. Measurements of formaldehyde at the U.S.–Mexico border during the Cal–Mex 2010 air quality study. *Atmospheric Environment* 70, 513–520.

Zheng, J., Garzon, J.P., Huertas, M.E., Zhang, R.Y., Levy, M., Ma, Y., Huertas, J.I., Jardon, R.T., Ruiz, L.G., Tan, H.B., Molina, L.T., 2013b. Volatile organic compounds in Tijuana during the Cal–Mex 2010 campaign: Measurements and source apportionment. *Atmospheric Environment* 70, 521–531.